

A TLD based method to estimate bowtie filter shape in PET/CT

N. Ahmadi¹, M.N. Nasrabadi¹, A. Karimian^{2*}, A. Rahmim³

¹Department of Nuclear Engineering, Faculty of Advanced Sciences & Technologies, University of Isfahan, Isfahan, Iran

²Department of Biomedical Engineering, University of Isfahan, Isfahan, Iran

³Department of Radiology and Department of Electrical & Computer Engineering Johns Hopkins University, Baltimore, MD21287, USA

ABSTRACT

Background: In CT systems, the machine utilizes a bowtie filter to shape the X-ray beam and remove lower energy photons. The shape of this bowtie filter is complicated and its geometry is often not available in detail. These renders the CT dose index (CTDI) to have different values in measurement versus Monte Carlo simulation studies and other analytical calculations especially in dosimetry of internal organs. In existing literature, the bowtie filter shape is extracted by using expensive sensors **Materials and Methods:** In the present work, the shape of the bowtie filter of the Biograph 6 PET/CT was derived by using Thermoluminescence dosimeters (TLDs). Subsequently, to evaluate the accuracy of the body bowtie filter shape as generated by TLDs, Monte Carlo simulation of CT was performed. 16 X-ray sources in various angles were used within the Monte Carlo code (MCNP-4C) to simulate the CT section of the PET-CT Biograph 6 system and to calculate dose. **Results:** The relative difference between simulated and measured CTDI value for the PET/CT Siemens Biograph 6 at 80, 110 and 130 kVp were 4.2, 2.9 and 2.3%, respectively. **Conclusion:** In this study, we demonstrate that it is possible to calculate the bowtie filter shape by using an inexpensive TLD method. The results showed that it is possible to determine the shape of the bowtie filter in PET/CT using TLDs with acceptable accuracy.

Keywords: PET/CT, bowtie filter, TLD dosimeter, dosimetry.

► Original article

*Corresponding authors:

Dr. Alireza Karimian,

Fax: +98 313 7932771

E-mail: karimian@eng.ui.ac.ir

Revised: March 2017

Accepted: April 2017

Int. J. Radiat. Res., October 2017;
15(4): 383-390

DOI: 10.18869/acadpub.ijrr.15.4.383

INTRODUCTION

Nowadays, CT systems are routinely used for PET machines by manufacturers for attenuation correction of the PET data, arriving at PET/CT system (1-3). The number of PET/CT scans performed has significantly increased in the past decade and the dose per patient has subsequently also increased from PET/CT systems (4-5). One of the most important issues of managing dose in the CT section of PET/CT is bowtie filter shaping that can be configured to absorb radiation from the x-ray source to control dose to body (4) by reducing the photon influence at the field of view (FOV) (7-8).

There are two types of bowtie filters for the CT scan: head and body bowtie filters. The shape of the bowtie filter, typically made of aluminum, is complicated and its manufacturers do not necessarily provide complete data about shape of the filter (6). The main role of X-ray beam shaping filtration including bowtie filters in the CT section is to balance the signal given variation of the body thickness across the transverse sections of the body and to reduce dose to the peripheral region of the body (2). The bowtie filter and beam collimation are used for multidetector CT (7).

The measurements of CT dose index (CTDI) value (8) and Monte Carlo simulation studies

could be different when the shape of bowtie filters is not provided by manufacturers especially in internal dosimetry. To estimate the shape of the bowtie filter, two general approaches have been utilized in few works. Computer simulations were developed and validated to determine the optimum bowtie filter for different patient sizes. A rectangle and an elliptical cutout simplified shape was assumed for the bowtie filter⁽⁴⁾. Bowtie filter shape was modeled by defining inflection parameter FW (Filter Isocenter and Width) from 1 to 9 for GE LightSpeed VCT. It should also be emphasized that the drawback of this method was utilizing a simple shape consisting a rectangle and an elliptical cutout and large image noise errors for diameter more than 35 cm⁽⁴⁾. Belinato *et al.*⁽⁹⁾ used the AGMS-D sensor (Accu-Gold kit Radcal Corporation) to estimate the bowtie filter shape of the Siemens Biograph 16 Truepoint and GE Discovery VCT PET/CT systems in 2015. They used 9 measurement points for estimating the bowtie filter by AGMS-D sensor for available kV in both systems. They showed approximately 4% difference between measurement and simulation CTDI₁₀₀ for kVp=110 at the center position⁽⁹⁾. Using this method for estimating the shape of body bowtie filter is relatively expensive due to the use of semiconductor sensor technology. Because of the small size of the sensor, for this dosimetry, 9 sensors simultaneously or doing dosimetry for 9 times should be employed.

In the present study, a body CTDI phantom (PMMA) was used for measuring CTDI_w. To simulate the CT section of the PET-CT Biograph 6 system, 16 X-ray sources were used in the Monte Carlo code for calculating dose.

The goal of this study is to introduce a new and inexpensive method to determine body bowtie filter shape of PET/CT (Biograph 6 Siemens Company) using Thermoluminescence Dosimeters (TLD). In the CT scan section of PET-CT machine, two types of bowtie filter are utilized; head bowtie filter and body bowtie filter. Teflon, PMMA or aluminum are common materials used for manufacturing the bowtie filter which the aluminum was selected. This study is focused to determine the real shape of

body bowtie filter by applying dosimetry method.

MATERIALS AND METHODS

Calculation of the bowtie filter shape using TLDs

Figure 1 shows the flow diagram to estimate the bowtie filter shape for CT component of the Biograph 6 PET/CT using TLDs. Box 1 and 2 of the diagram show that the TLDs chips are calibrated and set inside the PMMA.

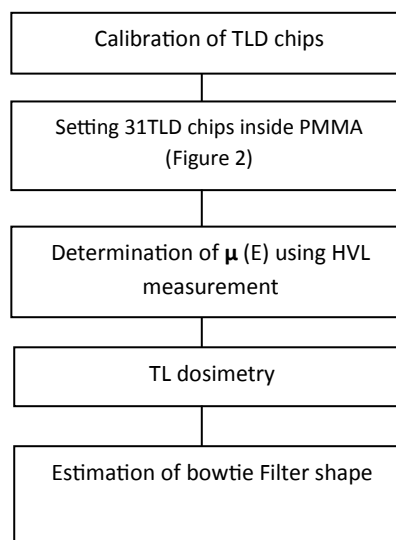


Figure 1. The used flow diagram to estimate the bowtie shape of CT of Biograph 6 Siemens PET/CT.

For calibration of TLD chips and setting, 31TLD chips (GR-200 series) made of LiF: Mg, Cu, and P were utilized. These chips have an extremely low detectable threshold and are near-air or tissue equivalent. The effective atomic number Z is 8.2, and it has a linear dose range 10⁻⁷ ~12 Gy.

All chips have circular shape with 4mm in diameter and 0.9 mm in thickness⁽¹⁰⁾. These chips calibrated by Cs-137 in SSDL organization and ECC (Element Correction Coefficient) of them have been reported in table1 using TLD reader Harshaw-4000. The outputs of TLD reader (nano-coulomb (NC)) were corrected by energy dependency response curve of LiF:Mg, Cu, P dosimeters⁽¹¹⁾.

Table 1. Element Correction Coefficient (ECC) resulting from TLD calibrated in SSDL organization according to the specified number of each TLD chip used in this study. Each TLD chips specified with a number from 1 to 31.

No. of TLDs	1	2	3	4	5	6	7	8	9	10	11	12	13	14	15	16
ECC	1.057	1.017	0.965	1.048	0.975	1.113	1.074	0.943	1.023	0.943	0.925	1.071	1.017	0.939	0.941	1.020
No. of TLDs	17	18	19	20	21	22	23	24	25	26	27	28	29	30	31	
ECC	1.119	0.967	0.963	1.015	0.986	0.936	0.913	1.024	0.934	1.068	1.052	0.929	0.917	0.904	0.917	

These TLD chips are placed in one slice of PMMA with 3 ×40 cm² dimensions and 4 mm thickness. This device has 31 holes with 6mm diameter and 2mm depth and 1 cm distance (figure 2).

This device is placed in 20 cm distance from the gantry isocenter to determine of body bowtie filter shape by TL dosimetry. The chip No.16 was located in the center of the axial field of view (FOV). The chips are arranged by laser in the gantry and the profile of CT machine is set to abdomen routine topogram by using kVp=110 and mA=100.

For determination of μ(E) using HVL measurement, transition X-ray photons through a bowtie filter were calculated using the standard attenuation equation 1:

$$I(E) = I_0(E) \exp \{-\mu_n(E)Y_n\} \quad (1)$$

μ_n (E) is the liner attenuation coefficient which depends on the energy. The X-ray photons from the CT scan have an energy spectrum I₀ (E) that could be listed by using the SRS-78 software or as obtained from physical models or

measurements. Y_n is thickness within the bowtie filter in the direction of the X-ray photons. For solving equation 1 and finding Y_n, μ (E) value was determined by using the following equation 2.

$$\mu = \frac{0.693}{HVL} \quad (2)$$

HVL value was calculated by experimental dosimetry via the ion chamber (Barracuda, RTI Electronics AB, 110 kVp)

The shape of the bowtie filter is thus estimated by knowing these parameters and utilizing equations 1 and 2. Y indicates the thickness of the bowtie filter where the energy is equal to 110 kVp, and μ is equal to 0.460. Therefore, I₀/I can be calculated by using the maximum value of entry dose to TLD chips in the middle of the bowtie filter and normalizing per each value of dose in other chips. Thus, the absorbed dose in each chip can indicate the thickness of bowtie filter in direction of X-ray photons. Figure 3 shows the arrangement of TLD chips and bowtie filter in X-ray FOV in this study.

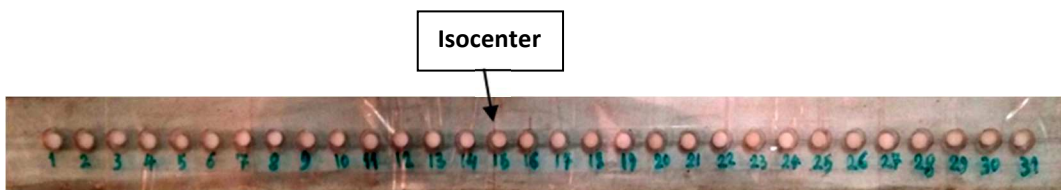


Figure 2. Arrangement of GR-200 TLD chips that are placed in a piece of PMMA with 3 ×40 cm² dimension and 4 mm thickness with index number for each TLD chips.

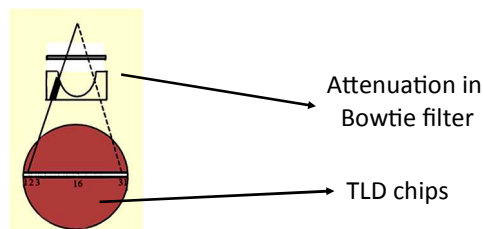


Figure 3. Schematic arrangement of TLD chips and the bowtie filter in X-ray FOV. The thickness of bowtie filter increases X-ray attenuation at peripheral points.

In this study, the PET-CT Biograph 6 from Siemens was considered (12). This system has 6 CT slices with 16 detector rows and 1472 channels per slice. DURA 422 MV is a type of X-Ray tube with 20-345 mA current tube and 80, 110 and 130kV for supporting tube voltages. The focal spot size according to IEC 60 366 is $0.8 \times 0.5/7^\circ$ and $0.8 \times 0.7/7^\circ$. The filtration information such as bowtie filter shape, according to our researches, was not easily presented by the manufacturer.

Experimental measurements and simulation of CTDI (PET/CT Biograph 6)

One of the most important aims of this study is to define the shape of bowtie filter that used in geometry section of Monte Carlo simulation program, which could be used for of CT section of PET-CT simulation. Figure 4 shows the flow diagram which is used to measure and simulate CTDI of CT section PET/CT biograph 6.

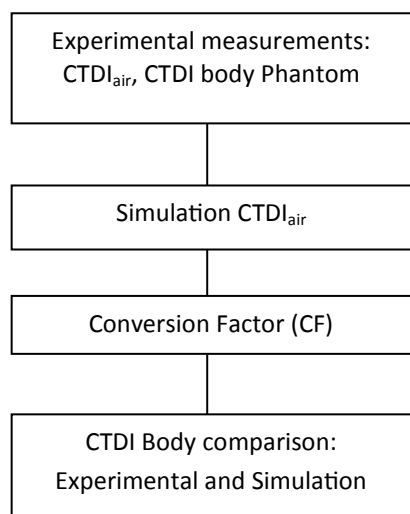


Figure 4. Experimental and simulation of CTDI_{air}, CTDI body Phantom.

For experimental measurement CTDI_{air}, ion chamber is located in center of FOV with pitch=1 and slice thickness=10 mm in mAs=100 for 80, 110, 130 KVp. Moreover, CTDI_w value was measured using body CTDI phantom with 15 cm length and 32 cm diameter. It was made of PMMA with of 1.19 gr.cm⁻³ density. There were holes that could use PMMA plug or pencil ion chamber. One hole was at the center and the other four holes were located 1 cm below the

phantom surface. Each hole has 90° distance from its neighbor (figure 5).

The ion chamber is placed serially in the

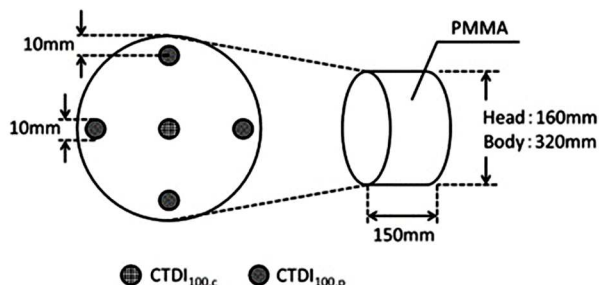


Figure 5. CTDI value is measured using 32 cm diameter was made of polymethylmethacrylate (PMMA) phantom.

center hole and the peripheral hole, and the measurements are combined to produce the weighted CTDI. The DCT 10 air ionization chamber model with flat energy response from RTI (Barracuda, RTI Electronics AB) was utilized for measuring CTDI_w.

To simulate CT section of PET/CT Biograph 6 system, 16 X-ray sources were used in Monte Carlo code (MCNP-4C) that are sufficient sources to approximate the continuous axial scan without significantly affecting the calculated dose. In the simulation code, absorbed dose was determined for CT scan with MeV/gram/source particle units and converted into absorbed dose with mGy/100 mAs units by conversion factor (CF) (9) using equation 3.

$$(CF)_E = \frac{CTDI(100, air, measured\ per\ 100\ mAs)}{CTDI(100, air, simulated\ per\ particle)} \quad (3)$$

The absorbed dose, in unit of mGy/100 mAs, was obtained by equation 4. $\sum N$ is the deposited energy in MeV/gram/source particle for all rotation during a PET/CT scan simulation (9):

$$D_{absolute} = D_{simulated} CF \sum N \quad (4)$$

In this method, we utilized 31 TLD chips that were located in one slice of PMMA in FOV and determined $\mu(E)$ (material attenuation coefficient) by measurement of the HVL value using ion chamber (Barracuda, RTI Electronics AB, 110KVp). According to the results of TLD dosimetry, we determined the thickness of bowtie filter and body bowtie filter shape of

PET/CT model Biograph 6 Siemens Company. The CTDIw values, obtained from measurement and simulation using this bowtie filter have been compared to each other.

The used data has been fitted by using equation 5, which indicates the shape of body bowtie filter. Figure 6 indicate shape of bowtie filter by X and Y are horizontal distance (cm) and the thickness of bowtie filter (mm Al), respectively)

RESULTS

In table 2, the results of nano-coulomb (NC) measurements from the TLD reader are presented in 2 rows. Also using data in table 1, the dose (ECC*NC) are determined (table 2). The thickness (Y_n) (n=1, 2, 3 ... 31 TLDs numbers) of bowtie filter was calculated by using equations 1 and 2 and has been shown in the 4th row of table 2.

$$Y = 0.0192x^2 - 0.6148x + 5.6564 \quad (5)$$

Graphical shape of body bowtie filter of PET/CT Biograph 6 (present study) is presented in figure 7a.

For simulation, the X-ray spectrum of sources that are used for CT section of PET/CT system for 80, 110 and 130 kVp is shown in figure 8, which is obtained from SRS-78 software with anode angle 7.0° and beam opening is 56°.

Table 2. Calculated results of NC (nano-coulomb), Element Correction Coefficient (ECC), ECC*NC and thickness(Y) of bowtie filter for Biograph 6 PET/CT system.

TLDS No(n)	1	2	3	4	5	6	7	8	9	10	11	12	13	14	15	16
NC	213.2	210.8	237.8	280.5	287.1	382.5	428.5	476.2	583.6	717.7	938.8	1157.7	1349.6	1238.4	1311.3	1166.6
ECC*NC	225.3	214.7	230.0	294.1	280.0	425.8	449.0	449.4	597.5	677.0	868.5	1240.4	1373.1	1163.0	1233.5	1190.3
Thickness(Y)	4.177	4.283	4.133	3.599	3.705	2.794	2.679	2.677	2.058	1.786	1.245	0.470	0.249	0.61	0.482	0.55
TLDS No(n)	17	18	19	20	21	22	23	24	25	26	27	28	29	30	31	
NC	1375.6	1182.2	1181.5	985.3	868.2	872.5	641.5	590.1	487.3	395.9	359.7	300.5	265.9	235.2	201.2	
ECC*NC	1540.5	1143.3	1138.0	1000.2	856.4	816.8	585.6	604.5	455.2	422.8	378.4	279.0	243.8	212.6	184.4	
Thickness(Y)	0.160	0.647	0.657	0.938	1.275	1.378	2.101	2.032	2.64	2.809	3.050	3.713	4.006	4.304	4.614	

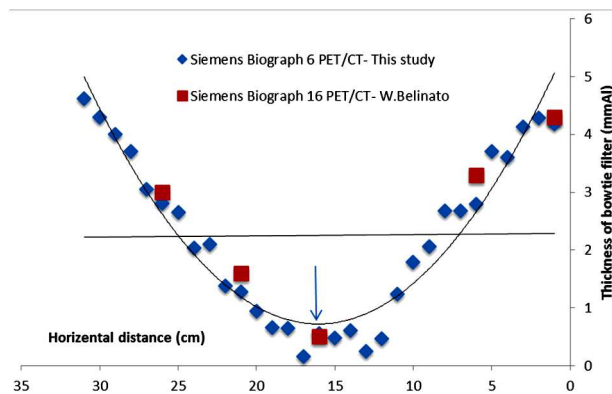


Figure 6. The results of body bowtie filters thicknesses of Siemens Biograph 6 PET/CT (present study) and Siemens Biograph 16 PET/CT in various areas of FOV.

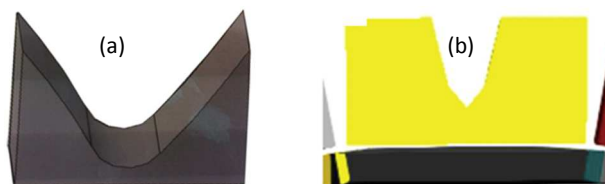


Figure 7. (a) The graphical Shape of body bowtie filter of PET/CT Biograph 6 (present study). (b) Body bowtie filter shape of Siemens Biograph 16 true point PET/CT that are estimated by using the Accu-Gold kit Radcal (Radcal Corporation, Monrovia, CA) with AGMS-Dsensorex.

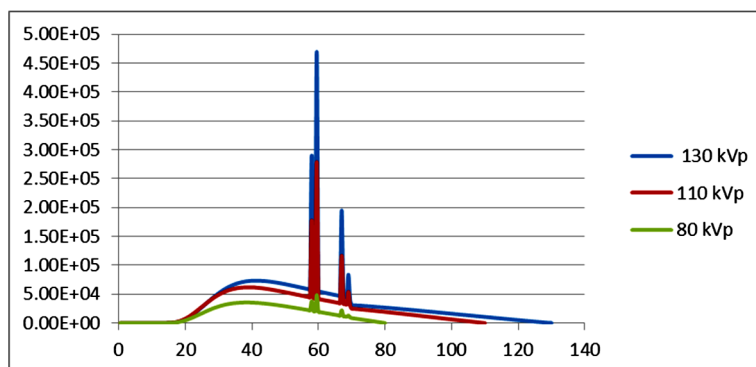


Figure 8. The X-ray spectra of sources that used for simulation CT section of PET-CT Biograph 6 system in 80, 110 and 130 kVp obtained from SRS-78 software.

The conversion factors (CF) obtained by simulation code and summarized in Table 3 that are obtained by simulation code where the simulation took into account 108 particles with the 80, 110 and 130 energies related to PET/CT Siemens biograph 6.

The relative difference between measurement (dm) and simulated (ds) CTDI was computed with equation 6 to obtain disparity

between the simulated and measured value:

$$\Delta_{rel} = \left| \frac{dm - ds}{dm} \right| \quad (6)$$

Table 4 and figure 9 show the results of the simulated and measured CTDIw values and relative difference for PET/CT Siemens Biograph 6 (our study) and Biograph 16 in 80, 110 and 130 kVp.

Table 3. Conversion factor obtained for PET/CT Siemens Biograph 6 (our presented work).

kVp	Beam collimation(mm)	Measured CTDI ₁₀₀ in air (mGy/100mAs)	Simulated CTDI ₁₀₀ in air (Mev/gram/particle)	Conversion factor (mGy gram particle/100mAs/Mev)
80	1×6.0	2.53	11.93E-9	2.12E+8
110	1×6.0	5.50	30.4E-9	1.8E+8
130	1×6.0	7.63	33.7E-9	2.26E+8

Table 3. Conversion factor obtained for PET/CT Siemens Biograph 6 (our presented work).

kVp	PET/CT Siemens Biograph 16	PET/CT Siemens Biograph 6 (our study)
	% Difference between Measured CTDI (mGy/100mAs) with Simulated (mGy/100mAs)	% Difference between Measured CTDI (mGy/100mAs) with Simulate (mGy/100mAs)
80	4.2	4.2
110	1.13	2.9
130	2.29	2.3

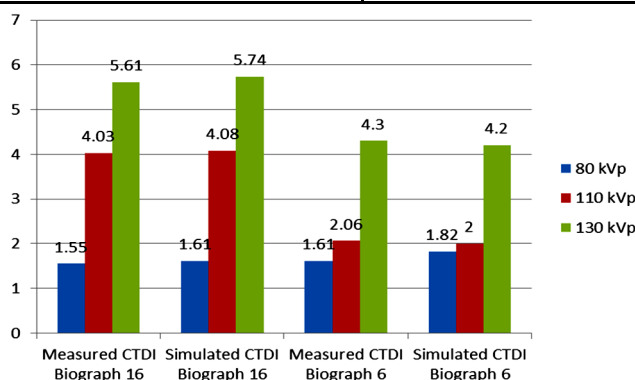


Figure 9. The measurements and simulated CTDIw (mGy/100mAs) values of the results of PET/CT Siemens Biograph 6 (our presented work) and Biograph 16.

DISCUSSION

The shape of bowtie filters from Siemens Company Biograph 16 true point ⁽¹³⁾ and Biograph 6 our study (figures 6, 7a and 7b) was compared and also results of measurements and simulated CTDI_w (mGy/100mAs) value and relative difference (figure 9), there is an excellent agreement in comparison of both body bowtie filter Biograph 16 true point and Biograph 6 PET/CT from Siemens Company.

The data of simulation code (MCNP-4C) with less than 5% error were generally reliable ⁽¹⁴⁾. Thus, simulation of CT section of PET/CT Siemens Biograph 6 (our presented work) with this shape of body bowtie filter (figure 7a) were validated with comparing difference values (Δ_{rel}) between the measurements and simulated CTDI_w (mGy/100mAs) in energies available (figure 9). Patient dose in CT systems is usually indicated in terms of organ dose and effective dose. According to significant correlation between CTDI_w and organ dose (ratio of organ dose to CTDI_w 1.37 ⁽¹⁵⁾) and results of CTDI value (figure 9), organs dose in PET/CT Biograph 6 were generally less than PET/CT biograph 16.

A dosimetry method to estimate body bowtie filter shape as applied to PET/CT scanner systems was presented and was compared with another frame work. The price range of each TLD chip is \$10-20 and accessible in most dosimetry divisions, compared with the range price \$ 3000-4000 of the Accu-Gold kit Radcal. The proposed method used TLD chips that are accessible and inexpensive whereas using the Accu-Gold kit Radcal system is significantly more expensive in comparison. For similar bowtie filter shapes of two PET/CT systems (this study vs. work by Belinato *et al.* ⁽⁹⁾) at kVp=110 and 100 mAs, the results show minimum errors between measurements and simulated CTDI_w(mGy/100mAs) values. In this study, body bowtie filter shape for a specific model of PET/CT system was determined and it could be utilized as input into the geometry section of relevant Monte Carlo simulation programs. Consequently, our study may help researchers determine, using very feasible means, the real value of CTDI with minimum

error between experimental measurements and Monte Carlo simulations, especially in dosimetry of internal organs.

Conflicts of interest: Declared none.

REFERENCES

1. Bushberg JT, Seibert JA, Leidholdt EM, Boone JM, Goldschmidt EJ (2003) The Essential physics of medical imaging. American Association of Physicists in Medicine; *Med Phys*, **30(7)**: 1936.
2. Gu J, Bednarz B, Caracappa PF, Xu XG (2009) The development, validation and application of a multi-detector CT (MDCT) scanner model for assessing organ doses to the pregnant patient and the fetus using Monte Carlo simulations. *Phys Med Biol*, **54(9)**: 2699–717.
3. Park HH, Park DS, Kweon DC, Lee SB, Oh KB, Lee JD, *et al.* (2011) Inter-comparison of 18F-FDG PET/CT standardized uptake values in Korea. *Appl Radiat Isot*, **69(1)**: 241–6.
4. Toth TL, Cesmeli E, Ikhlef A, Horiuchi T (2005) Image quality and dose optimization using novel x-ray source filters tailored to patient size. In: *Flynn MJ, editor*. 283.
5. Fan J, Pack JD, Cao GD (2016) Systems and methods for adjustable view frequency computed tomography imaging. U.S. Patent No. 20,160,038,113. 14/451616.
6. Panetta D (2016) Advances in X-ray detectors for clinical and preclinical Computed Tomography. *Nucl Instruments Methods Phys Res Sect A Accel Spectrometers, Detect Assoc Equip*, **809**: 2–12.
7. Angel E, Wellnitz C V, Goodsitt MM, Yaghmai N, DeMarco JJ, Cagnon CH, *et al.* (2008) Radiation dose to the fetus for pregnant patients undergoing multidetector CT imaging: Monte Carlo simulations estimating fetal dose for a range of gestational age and patient size. *Radiology*, **249(1)**: 220–7.
8. Jessen KA, Shrimpton PC, Geleijns J, Panzer W, Tosi G (1999) Dosimetry for optimisation of patient protection in computed tomography. *Appl Radiat Isot*, **50(1)**: 165–72.
9. Belinato W, Santos WS, Paschoal CMM, Souza DN. (2005) Monte Carlo simulations in multi-detector CT (MDCT) for two PET/CT scanner models using MASH and FASH adult phantoms. *Nucl Instruments Methods Phys Res Sect A Accel Spectrometers, Detect Assoc Equip*, **784**: 524–30.
10. GR-200 TLD. Available from: <http://www.csimc-freqcontrol.com/products4.html>
11. Carinou E, Boziari A, Askounis P, Mikulis A, Kamenopoulou V (2008) Energy dependence of {TLD} 100 and MCP-N detectors. *Radiat Meas*, **43(2–6)**: 599–602.
12. Jakoby BW, Bercier Y, Conti M, Casey ME, Bendriem B, Townsend DW (2011) Physical and clinical performance of the mCT time-of-flight PET/CT scanner. *Phys Med Biol*, **56(8)**: 2375–89.
13. Belinato W, Santos WS, Paschoal CMM, Souza DN (2013)

Monte Carlo simulations in multi-detector CT (MDCT) for two PET/CT scanner models using MASH and FASH adult phantoms. *Nucl Instruments Methods Phys Res Sect A Accel Spectrometers, Detect Assoc Equip*, **784**: 524–30.

14. Briesmeister JF (2000) MCNP4C: Monte Carlo N-particle transport code system. MCNP-4C Monte Carlo N-Particle

Transp Code Syst.

15. Hidajat N, Mäurer J, Schröder RJ, Nunnemann A, Wolf M, Pauli K, *et al.* (1999) Relationships between physical dose quantities and patient dose in CT. *Br J Radiol*, **72(858)**: 556–61.